The Astrophysical Journal Letters, 890:L15 (5pp), 2020 February 20 https://doi.org/10.3847/2041-8213/ab72fe

Spontaneous Onset of Collisionless Magnetic Reconnection on an Electron Scale

Dongkuan Liu[1,2], San Lu[3], Quanming Lu[1,2], Weixing Ding[1,2], and Shui Wang[1,2]
[1] CAS Key Laboratory of Geospace Environment, Department of Geophysics and Planetary Science, University of Science and Technology of China, Hefei, Anhui, People's Republic of China; qmlu@ustc.edu.cn
[2] CAS Center for Excellence in Comparative Planetology, People's Republic of China
[3] Department of Earth, Planetary, and Space Sciences and Institute of Geophysics and Planetary Physics, University of California, Los Angeles, CA, USA slu@igpp.ucla.edu
Received 2019 December 3; revised 2020 January 31; accepted 2020 February 5; published 2020 February 14

Abstract

Using particle-in-cell simulations, we investigate the onset of magnetic reconnection from a quiescent Harris current sheet in collisionless plasmas. After the current sheet is destabilized by the collisionless tearing mode instability, it proceeds to onset of reconnection, which manifests spontaneous thinning of current sheet and pileup of upstream magnetic flux. Once the current sheet thins to a critical thickness, about two electron inertial lengths, reconnection begins to grow explosively in this electron current sheet. This study shows that the spontaneous onset of collisionless magnetic reconnection is controlled by electron kinetics.

Unified Astronomy Thesaurus concepts: Solar magnetic reconnection (1504); Plasma physics (2089); Heliosphere (711); Planetary magnetosphere (997)

1. Introduction

Magnetic reconnection (Birn & Priest 2007; Yamada et al. 2010; Wang & Lu 2019), a process that converts magnetic energy to plasma energy via topological changes in magnetic field lines, is widely believed to cause explosive phenomena in various plasma environments throughout the universe, including collisional (e.g., magnetar flares and solar chromosphere) and collisionless (e.g., solar corona, solar wind, and Earth's magnetosphere) plasmas. The occurrence of magnetic reconnection requires a dissipation mechanism, which is provided by collisional resistivity in collisional plasmas (Parker 1957; Sweet 1958; Loureiro et al. 2007; Bhattacharjee et al. 2009; Pucci & Velli 2014). In collisionless plasmas, however, the dissipation mechanism needs to rely on particle kinetic effects (Vasyliunas 1975; Cai & Lee 1997; Hesse et al. 1999; Pritchett 2001; Ricci et al. 2002; Wang & Lu 2019).

It has been well recognized that collisionless magnetic reconnection has a fast reconnection rate, on the order of 0.1 (Birn et al. 2001; Liu et al. 2017). However, the transition from a quiescent state to such a fast reconnection, that is, the onset of collisionless magnetic reconnection, has been poorly understood. Although it has been proposed that the collisionless magnetic reconnection can be initiated by a collisionless tearing mode instability through electron Landau resonance (e.g., Coppi et al. 1966; Drake & Lee 1977; Pritchett et al. 1991), the linear growth of this instability saturates at a very low rate, much lower than 0.1, with insignificant magnetic topological changes (Katanuma & Kamimura 1980; Lu et al. 2013a, 2019). Therefore, how the current sheet evolves from the tearing mode instability to fast growing reconnection is unknown. To fill this knowledge gap, we study such evolution using particle-in-cell simulations.

2. Simulation Model and Results

The simulations are performed in a two-dimensional box in the x–z plane, $[0, L_x] \times [-L_z/2, L_z/2]$. The initial configuration is the Harris current sheet with the magnetic field $\boldsymbol{B} = B_0 \tanh(z/\delta_0)\boldsymbol{e}_x$ and the plasma density $n = n_b + n_0 \,\mathrm{sech}^2(z/\delta_0)$. Here B_0 is the asymptotical magnitude of the magnetic field, δ_0 is the half-thickness of the current sheet, n_0 is the current sheet peak density, and n_b is the background density. The background density is $n_b = 0.2n_0$, and uniform electron and ion temperatures are adopted, with $T_i/T_e = 4$. The size of the simulation box is $L_x = L_z = 50d_i$, where d_i is the ion inertial length defined by n_0. Periodic boundary conditions are adopted in the x direction, and perfect conductor boundary conditions are used in the z direction. We consider cases with different values of the initial current sheet half-thickness δ_0 and ion-to-electron mass ratio m_i/m_e, as listed in Table 1. In the simulations, magnetic reconnection occurs spontaneously, i.e., it is not initialized by any artificial perturbations.

Figure 1(a) shows magnetic field evolution for Case 0 (the standard case with $\delta_0 = 0.5d_i$ and $m_i/m_e = 100$). Magnetic reconnection with the quadrupolar out-of-plane magnetic field B_y (Shay & Drake 1998; Hoshino et al. 2001; Pritchett 2001; Ren et al. 2005; Fu et al. 2006; Eastwood et al. 2010) emerges at about $\Omega_i t = 30$ and becomes better developed at $\Omega_i t = 35$. The Harris current sheet is destabilized by the collisionless tearing mode instability (Katanuma & Kamimura 1980; Pritchett et al. 1991; Lu et al. 2013a, 2019), and the linear growth of this instability saturates at about $\Omega_i t = 13$, with little reconnected flux $\Delta\psi \approx 0.01$ (not shown). Rapid growth of magnetic reconnection begins from about $\Omega_i t = 33$ with $\Delta\psi \approx 0.1$ (Figure 1(b)). In this Letter, we study the transition from the linear growth of collisionless tearing to fast reconnection, so we focus on the time period from $\Omega_i t = 13$ to 33 (the shaded period in Figure 1(b)).

Figure 2(b) shows the z profile of the magnetic flux function deviated from its initial value (Figure 2(a)), $\psi_1 = \psi - \psi_0$, at the reconnection site, $x = 22.8d_i$. From $\Omega_i t = 13$ to 33, the magnetic flux increases at current sheet center, indicating the onset of reconnection. A double-peaked structure of the perturbed magnetic flux ψ_1 is formed, which is consistent with the analysis of resistive tearing mode instability (e.g., Biskamp 2000; Loureiro et al. 2007). This double-peaked structure of ψ_1 suggests that there is a pileup of magnetic flux in the upstream during this time. The reconnection rate (Figure 1(b)) at this time is much lower than 0.1, too slow to reconnect the inflowing magnetic flux

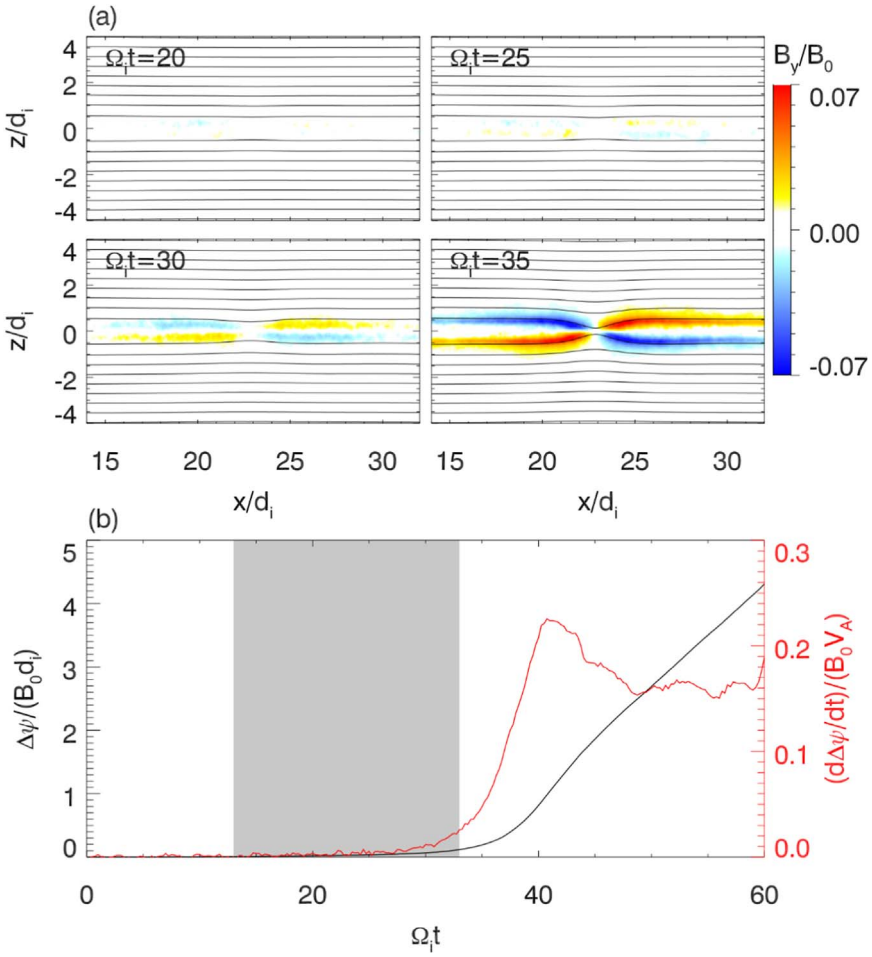

Figure 1. For Case 0. (a) Evolution of in-plane magnetic field lines and out-of-plane magnetic field B_y/B_0 during the onset process. (b) Time histories of reconnected magnetic flux $\triangle\psi$ and reconnection rate $d\triangle\psi/dt$. Here the reconnected magnetic flux $\triangle\psi$ is in units of $B_0 d_i$, and it is defined as the difference between the maximum and minimum of ψ at $z = 0$. The reconnection rate $d\triangle\psi/dt$ is in units of $B_0 V_A$, and it is equivalent to the magnitude of reconnection electric field E_y at the reconnection site. In this study, we focus on the onset period (gray) covering the transition from the collisionless tearing mode instability ($\Omega_i t = 13$) to fast growth of reconnection ($\Omega_i t = 33$).

timely, so the flux is piled up in the upstream region. The value of the reconnection rate $d\triangle\psi/dt$ is equivalent to the magnitude of the reconnection electric field at the reconnection site, and this electric field (although weak) gradually accelerates the electrons and decelerates the ions in the y direction, leading to an increase in electron current density (Figure 2(d)) and a decrease in ion current density (Figure 2(c)). Such current density redistribution forms an electron current sheet at the reconnection site, and the thickness of this electron current sheet decreases at the same time (Figure 2(c)).

This current sheet thinning is further demonstrated in Figure 3. In Case 0, the current sheet half-thickness decreases from its initial value $0.5d_i$ to about $0.18d_i$ at $\Omega_i t = 33$; after this critical point, reconnection begins to proceed rapidly. This feature is examined using more cases with different initial values of current sheet thickness (Cases 1, 2, and 3). As shown in Figure 3(a), for all these cases, the current sheet thinning also stops at the critical value $\delta_c = 0.18d_i$, and then the thickness increases during the fast reconnection stage. Note that this critical thickness $0.18d_i$ is equivalent to $1.8d_e$, where d_e is the electron inertial length evaluated using the mass ratio $m_i/m_e = 100$. We further examine whether δ_c is controlled by electron kinetics or ion kinetics using two more cases with different mass ratios (Cases 4 and 5; note that we only change the electron mass and leave the ion mass unchanged). As shown in Figure 3(b), in Case 4 ($m_i/m_e = 25$), $\delta_c = 0.3d_i = 1.5d_e$, and in Case 5 ($m_i/m_e = 400$), $\delta_c = 0.105d_i = 2.1d_e$. Although δ_c varies in units of d_i, it is invariably about $2d_e$ in all the cases, indicating that the current sheet thinning is controlled by electron kinetics.

Table 1
Simulation Parameters for the Cases Considered

Case	δ_0/d_i	m_i/m_e	$\triangle/d_i$	c/V_A
0	0.5	100	0.05	15
1	0.4	100	0.05	15
2	0.6	100	0.05	15
3	0.7	100	0.05	15
4	0.5	25	0.1	7.5
5	0.5	400	0.025	30

Note. Here $\triangle$ is the grid size, c is the speed of light, and V_A is the Alfvén speed evaluated using B_0 and n_0. Note that $\triangle/d_i$ and c/V_A vary with m_i/m_e to maintain λ_{De}/Δ and ω_{pe}/Ω_e, where λ_{De} is the Debye length, ω_{pe} is the electron plasma frequency, and Ω_e is the electron gyrofrequency.

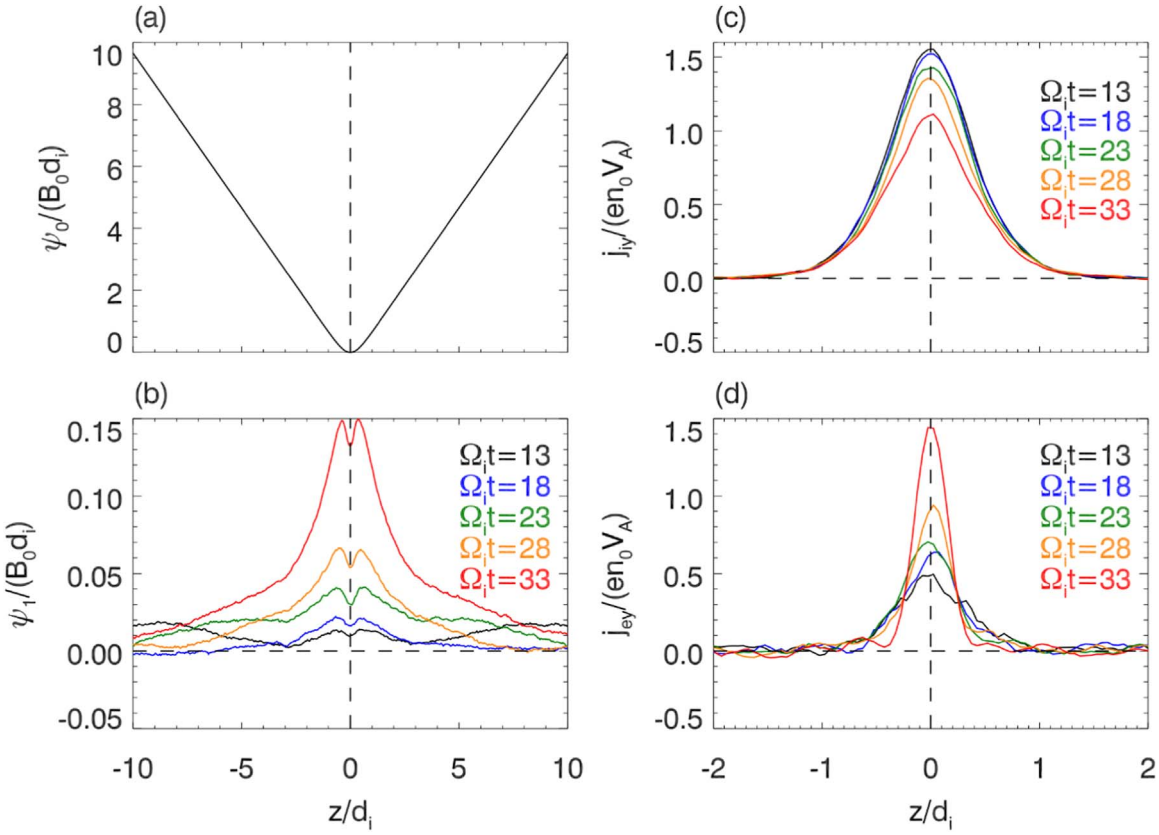

Figure 2. For Case 0 at the reconnection site $x = 22.8d_i$. The z profile of (a) the initial magnetic flux $\psi_0 = B_0\delta_0 \ln[\cosh(z/\delta_0)]$ and the z profiles of (b) perturbed magnetic flux $\psi_1 = \psi - \psi_0$, (c) out-of-plane ion current density j_{iy}, and (d) out-of-plane electron current density j_{ey} at representative moments. The magnetic flux is in units of B_0d_i, and the current densities are in units of en_0V_A.

3. Conclusions and Discussion

To conclude, after reconnection is initiated by collisionless tearing mode instability, magnetic flux piles up in the upstream region because the reconnection rate at this time is too slow to dissipate the inflowing magnetic flux. This pileup is accompanied by spontaneous current sheet thinning of the reconnecting current sheet to a critical thickness, about two electron inertial lengths. After this critical point, reconnection begins its fast growth in this electron scale thin current sheet.

Current sheet thinning and the pileup of upstream magnetic flux usually occur in externally driven scenarios of magnetic reconnection, such as reconnection in laser-produced plasmas (Nilson et al. 2006; Li et al. 2007; Fox et al. 2011; Lu et al. 2013b) and storm/substorm-time reconnection in Earth's magnetotail (Hesse & Schindler 2001; Pritchett 2010; Liu et al. 2014; Pritchett & Lu 2018). We are surprised to find that in our simulations, the upstream magnetic flux piles up and the current sheet thins spontaneously during the onset of reconnection, even without any external driver. In this onset process, the reconnection rate is low, which is insufficient to dissipate the upstream magnetic flux timely. Therefore, the magnetic flux is piled up in the upstream region, which compresses and thins the current sheet. After the onset, in the fast reconnection stage, because the reconnection rate is high enough to dissipate the upstream magnetic flux, the flux stops piling up, which stops the current sheet thinning.

The current sheet stops thinning after the onset and becomes thicker during fast reconnection (see Figure 3). One possible reason responsible for this increase in current sheet thickness is that fast reconnection demands a large aspect ratio δ/L (e.g., Liu et al. 2017), where δ is the current sheet thickness, and L is the current sheet length. The reconnection current sheet is elongated in the fast reconnection stage (e.g., Daughton et al. 2006), corresponding to an increase in L. The system would self-consistently increase δ to keep the large aspect ratio so that the fast reconnection rate is maintained. During fast reconnection, the reconnection current sheet also becomes bifurcated with double-peaked current density in the out-of-plane direction (e.g., Gosling & Szabo 2008; Liu et al. 2013), which further complicates the issue of current sheet thickness. Other factors, such as boundary conditions and the magnitude of the guide field, may also affect the evolution of the reconnection current sheet. In this paper, we focus on the onset of fast reconnection; the issue of current sheet thickening in the fast reconnection stage is out of the scope of this paper and deserves a closer examination in a separate study.

We use PIC simulations, which resolve both electron and ion kinetics, to study collisionless magnetic reconnection in the Harris current sheet. The entire process includes three stages: (1) the Harris current sheet is first destabilized by collisionless tearing mode instability (e.g., Coppi et al. 1966), (2) then it evolves into the onset stage of collisionless reconnection, and (3) eventually it proceeds to the fast reconnection stage. In this paper, we only focus on the second stage, the onset of collisionless reconnection. In addition to the PIC simulations, hybrid simulations, which only resolve ion kinetics and treat electrons as a massless fluid, can also well describe the third

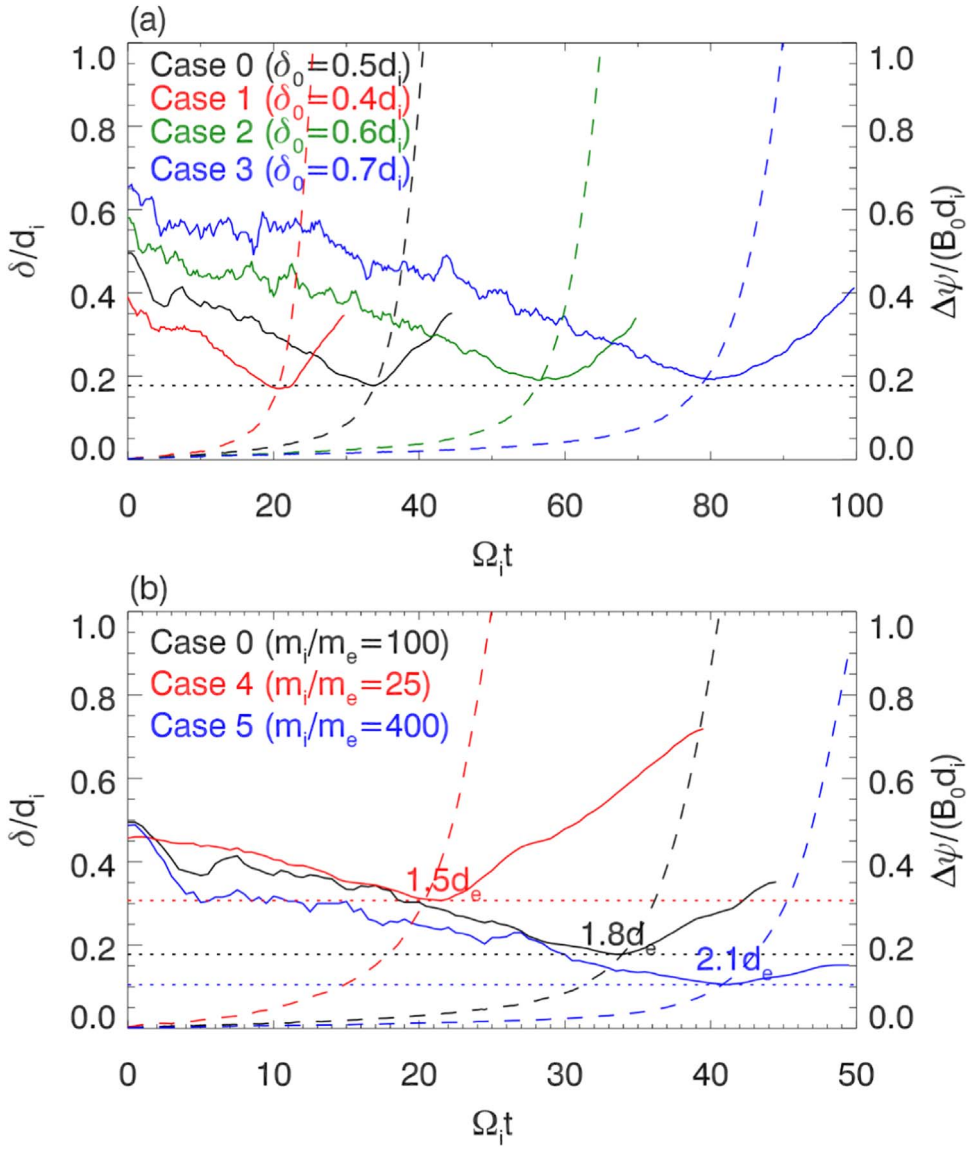

Figure 3. (a) Time histories of reconnecting electron current sheet half-thickness δ (solid lines) and reconnected flux $\triangle\psi$ (dashed lines) for cases with different values of (a) initial half-thickness δ_0 (Cases 0, 1, 2, and 3) and (b) mass ratio m_i/m_e (Cases 0, 4, and 5). Here δ is the half width at the half maximum of the electron current density's z profile at the reconnection site. In these cases, one or multiple X-lines are formed in the current sheet. In the case(s) with multiple X-lines, the definition of the reconnected flux $\triangle\psi$ as the difference between the maximum and minimum of ψ at $z = 0$ indicates that the best developed single X-line with ψ maximum is considered.

stage above, i.e., collisionless fast reconnection (e.g., Shay et al. 2001; Malakit et al. 2009; Le et al. 2016) because it has been shown that the fast reconnection process is controlled by ion kinetics (Hesse et al. 1999; Ricci et al. 2002). Here our PIC simulations show that the onset of the fast reconnection (the second stage above), however, is controlled not by ion kinetics but by electron kinetics. In hybrid simulations, to allow the onset of the collisionless fast reconnection in the absence of electron kinetics, an artificial resistivity is adopted to mimic the electron kinetics (so the resistivity is also called anomalous resistivity). If the artificial resistivity represents the anomalous resistivity caused by electron kinetics well, hybrid simulations can still be used to describe the onset of reconnection, but the description is not self-consistent like in PIC simulations because the resistivity is artificially given. Therefore, PIC simulation is demanded to fully resolve the onset of collisionless reconnection.

This work was supported by the NSFC grants 41527804, 41774169, Key Research Program of Frontier Sciences, CAS (QYZDJ-SSW-DQC010), and the B-type Strategic Priority Program of the Chinese Academy of Sciences (41000000). We thank Y. D. Jia and A. V. Artemyev for insightful discussion.

ORCID iDs

San Lu https://orcid.org/0000-0003-2248-5072
Quanming Lu https://orcid.org/0000-0003-3041-2682

References

Bhattacharjee, A., Huang, Y. M., Yang, H., & Rogers, B. 2009, PhPl, 16, 112102
Birn, J., Drake, J. F., Shay, M. A., et al. 2001, JGR, 106, 3715
Birn, J., & Priest, E. 2007, Reconnection of Magnetic Fields (New York: Cambridge Univ. Press)

Biskamp, D. 2000, Magnetic Reconnection in Plasmas (Cambridge: Cambridge Univ. Press)
Cai, H. J., & Lee, L. C. 1997, PhPl, 4, 509
Coppi, B., Laval, G., & Pellat, R. 1966, PhRvL, 16, 1207
Daughton, W., Scudder, J., & Karimabadi, H. 2006, PhPl, 13, 072101
Drake, J. F., & Lee, Y. C. 1977, PhFl, 20, 1341
Eastwood, J. P., Phan, T. D., Oieroset, M., & Shay, M. A. 2010, JGRA, 115, A08215
Fox, W., Bhattacharjee, A., & Germaschewski, K. 2011, PhRvL, 106, 215003
Fu, X. R., Lu, Q. M., & Wang, S. 2006, PhPl, 13, 012309
Gosling, J. T., & Szabo, A. 2008, JGR, 113, A10103
Hesse, M., & Schindler, K. 2001, EP&S, 53, 645
Hesse, M., Schindler, K., Birn, J., & Kuznetsova, M. 1999, PhPl, 6, 1781
Hoshino, M., Mukai, T., Terasawa, T., & Shinohara, I. 2001, JGR, 106, 25979
Katanuma, I., & Kamimura, T. 1980, PhFl, 23, 2500
Le, A., Daughton, W., Karimabadi, H., & Egedal, J. 2016, PhPl, 23, 032114
Li, C. K., Séguin, F. H., Frenje, J. A., et al. 2007, PhRvL, 99, 055001
Liu, Y. H., Birn, J., Daughton, W., Hesse, M., & Schindler, K. 2014, JGRA, 119, 9773
Liu, Y. H., Daughton, W., Karimabadi, H., Li, H., & Roytershteyn, V. 2013, PhRvL, 110, 265004
Liu, Y. H., Hesse, M., Guo, F., et al. 2017, PhRvL, 118, 085101
Loureiro, N. F., Schekochihin, A. A., & Cowley, S. C. 2007, PhPl, 14, 100703
Lu, Q. M., Lu, S., Huang, C., Wu, M. Y., & Wang, S. 2013a, PPCF, 55, 085019
Lu, S., Angelopoulos, V., Artemyev, A., et al. 2019, ApJ, 878, 109
Lu, S., Lu, Q. M., Dong, Q. L., et al. 2013b, PhPl, 20, 112110
Malakit, K., Cassak, P. A., Shay, M. A., & Drake, J. F. 2009, GeoRL, 36, L07107
Nilson, P. M., Willingale, L., Kaluza, M. C., et al. 2006, PhRvL, 97, 255001
Parker, E. N. 1957, JGR, 62, 509
Pritchett, P. L. 2001, JGR, 106, 3783
Pritchett, P. L. 2010, JGRA, 115, A10208
Pritchett, P. L., Coroniti, F. V., Pellat, R., & Karimabadi, H. 1991, JGR, 96, 11523
Pritchett, P. L., & Lu, S. 2018, JGRA, 123, 2787
Pucci, F., & Velli, M. 2014, ApJL, 780, L19
Ren, Y., Yamada, M., Gerhardt, S., et al. 2005, PhRvL, 95, 055003
Ricci, P., Lapenta, G., & Brackbill, J. U. 2002, GeoRL, 29, 2088
Shay, M. A., & Drake, J. F. 1998, GeoRL, 25, 3759
Shay, M. A., Drake, J. F., Rogers, B. N., & Denton, R. E. 2001, JGR, 106, 3759
Sweet, P. A. 1958, in IAU Symp. 6, Electromagnetic Phenomena in Cosmical Physics, ed. B. Lehnert (Cambridge: Cambridge Univ. Press), 123
Vasyliunas, V. M. 1975, RvGSP, 13, 303
Wang, S., & Lu, Q. M. 2019, Collisionless Magnetic Reconnection (Beijing: Science Press)
Yamada, M., Kulsrud, R., & Ji, H. T. 2010, RvMP, 82, 603